Adsorptive characteristics and performance of template-containing MCM-41 for removal of sodium dodecylbenzene sulfonate from aqueous solutions

Sedigheh Akbari Bengar*, Mohammad Ali Zanjanchi*, Shabnam Sohrabnezhad

Department of Chemistry, Faculty of Science, University of Guilan, P.O. Box: 41335-1914, Rasht, Iran, Tel./Fax: +98 1313233262; emails: sedigh3470@gmail.com (S.A. Bengar), zanjanchi@guilan.ac.ir (M.A. Zanjanchi)

ABSTRACT

The as-synthesized MCM-41 and its modified forms were studied as effective adsorbents for the removal of sodium dodecylbenzene sulfonate (SDBS) from contaminated aqueous solutions. The structure-directing template molecules of the as-synthesized MCM-41 was partially removed by treating the sample with an alcoholic ammonium nitrate solution through step by step procedure. The adsorbents were characterized using standard solid-state techniques such as X-ray diffraction, Fourier-transform infrared, Brunauer–Emmett–Teller, thermogravimetric analysis, and transmission electron microscopy. Optimization experiments were carried out as a function of pH, contact time, and the adsorbent dosage. The kinetics of the adsorption were well-described by the pseudo-second-order kinetic. The adsorption data were shown to be fitted with the Langmuir isotherm equation. The maximum adsorption capacities and pseudo-second-order rate constants were calculated. The efficiency of the adsorbents for removal of SDBS fluctuates with the amount of the template molecules retained in the mesoporous structures. Thermodynamic studies depicted that the adsorption of the surfactant is an endothermic process and it is controlled by entropy changes. The recycling of the adsorbent was studied, and the adsorption efficiency is significant even after three cycles of use. Ability of the adsorbent for removal of SDBS in real samples was also investigated.

Keywords: Sodium dodecylbenzene sulfonate; MCM-41; Adsorption; Template

1. Introduction

Surfactants are recognized for their fascinating properties which makes them suitable as detergents and cleaning products. Moreover, because of their promising peculiarity, these synthetic chemicals are significantly used in different fields including technological aspects and research areas in pharmacy, textile, cosmetics, agriculture, and biotechnology. Anionic surfactants are among the most common surfactants which were used prior to the others. They are habitually called the "workhorse" in the world of detergents because they are found in nearly all cleaners. Therefore, they are produced in large amounts and most of them are not costly [1]. Anionic surfactants commonly include either ester sulfate or sulfonated groups. These surfactants, owing to their large consumption worldwide in different industries and household uses, are released in large amounts into aquatic and global environments.

The presence of surfactants in aqueous systems can affect the biological wastewater cure processes. They cause difficulties in sewage aeration and treatments due to their high foaming, lower oxygenation potentials, and killing of waterborne organisms. They can be harmful to living species as well [2]. Therefore, the extent of surfactant species in wastewaters specifically those from textile and detergent manufacturers, are required reduced to safe levels prior to discharging them into the environment. These kinds of the treatments for wastewater should be taken seriously to protect public health [3]. A common method for the

* Corresponding authors.

refinement of polluted waters is biodegradation of surfactants. However, certain surfactant species may be stable to biodegradation or they are non-degradable species in nature [4]. Consequently, other common methods may be employed for removal or destruction of anionic surfactants from wastewaters. There is a variety of methods including chemical or electrochemical oxidation [5,6], membrane technology [7], ion exchange [8] adsorption [9], chemical precipitation [10], photocatalytic degradation [11], coagulation and flocculation [12,13], various biological methods [14,15], and aqueous two-phase PEG-salt systems [16].

Adsorption is considerably the most widely applied method among others. For efficient removal of surfactant, the high capacity of the adsorbent is very important. Adsorption processes are popular in chemical industries and environmental applications due to low operational and energy expenses [17]. One of the main factors for selecting or preparing an efficient adsorbent is to gain a high capacity of the adsorbent for the adsorbate. Various adsorbents have been implemented for the removal of anionic surfactants. These adsorbents include multiwalled carbon nanotubes [18], zero-valent iron nanoparticles [19], activated carbon [20], resins [21], metal oxides [22], chitosan [23], akaganeite [24], montmorillonite [25], organophylic bentonite [26], modified zeolite [27], carbonate rock [28], polyvinyl chloride latex [29], and MCM-41 [30]. Among them, the porous materials such as activated carbon or mesoporous MCM-41 are distinctive because they provide a very high capacity due to their large pores and huge surface area. The MCM-41 contains one-dimensional hexagonal channels with uniform size and with a pore diameter between 1.5 and 10 nm [31,32]. Due to its high specific surface area (1,000–1,500 $m^2 g^{-1}$) and tunable pore size, MCM-41 is capable of adsorbing various pollutants in water [32,33]. The thermal stability and low water affinity permit the high recycle potential of these mesoporous materials [33]. Despite all these advantages, MCM-41 is lacking efficient binding groups in its structure. A common technique to create adsorption sites into its structure is to modify its surface with functional groups [34]. But, performing this method needs paying for the expensive cost of functionalizing chemicals. Also, employing extra treatments such as functionalization usually reduces the structured ordering of MCM-41.
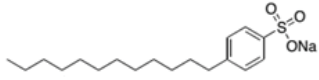
Another possibility to get a profit from the enormous capacity of the ordered mesoporous MCM-41, is the use of template containing MCM-41. In this condition, the cationic surfactant molecules, which are present in the structure, forms micellar phases inside the channels of the as-synthesized MCM-41. These micelles in the mesopore spaces provide the hydrophobic areas which are proper media for the sorption of organic species [35]. The studies on the sensor application [36], host-guest interactions [37], extraction behavior [38], and sorption properties [39] of surfactant-containing MCM-41 have been reported. In our earlier work, we found that by expelling out part of the cationic template (CTAB) from the synthesized MCM-41 through ion-exchange procedure, suitable free spaces would be created [30]. It was said that by this treatment, the bilayers of cationic structure-directing surfactant are formed as admicelles inside the pores. This leads to formation of positive charges on the surface of MCM-41 [30].

Therefore, the anionic contaminant species encounter a strong electrostatic interaction following the solubilization into the hydrophobic space of admicelles. On the other hand, in the as-synthesized sample only a monolayer of surfactants (called as hemimicelle) is formed on the surface. In this condition, the hemimicelles are responsible for the hydrophobic interactions between the organic pollutant and the surface. Thus, in both of the as-synthesized and the modified MCM-41 potential adsorbing sites are developed. But, there is an advantage for the modified forms, which in these samples the hydrophobic and electrostatic interactions are combined. This causes the adsorption capacity for the partial template-containing MCM-41 to be significantly enhanced.

Linear alkylbenzene sulfonates (LAS) are highly water soluble anionic surfactants and are widely used in synthetic laundry detergent formulations and household cleaning products. At present, LAS is considered to be a primary constituent in many liquid and powdered detergents. It is not expensive and its performance is approved so that makes LAS ideal for detergent applications. LAS have gained the alkyl chain from C-10 to C-14. After use and discharging into waterways these compounds can be source of significant environmental pollution. Their biodegradation includes the consumption of bio-available oxygen (BOD) which results in an increase in chemical oxygen demand (COD). So, these surfactants can greatly affect the aquatic environment and change the physiological properties of water [40]. The sodium dodecylbenzene sulfonate (SDBS) which is shown as the C-12 type of LAS is the subject of the present study. Its structure and features is demonstrated in Table 1.

This work is an extension of our earlier work carried out in our laboratory so far for removal of sodium dodecyl sulfate (SDS) [30]. From a chemical perspective, there is a significant diversity between the alkylsulfates and the alkylsulfonates. In the alkylsulfates, the sulfur atom is linked to the carbon chain via an oxygen atom. However, in the alkylsulfonates, the sulfur atom is directly bonded to carbon atom. The C–S bond weakens the tendency of sulfonates for hydrolysis. Also, from a surface activity viewpoint SDBS has lower CMC level than SDS. However, the important point is that SDBS is more harmful than SDS based on the LD_{50} value. The environmental and public health regulatory organizations have defined strict limits for anionic surfactants as 0.5 mg L^{-1} for drinking water and 1.0 mg L^{-1} for

Table 1
Structure and other chemical features of SDBS

Chemical structure	
Chemical formula	$C_{18}H_{29}NaO_3S$
Full chemical name	Sodium dodecylbenzene sulfonate
Molecular weight (g mol^{-1})	348.48
CMC (mM)	1.6
LD_{50}	2.3 mg L^{-1}

CMC: critical micelle concentration; LD_{50}: lethal dose, 50%.

other purposes [22]. Due to all these reasons, elimination and removal of SDBS from aqueous systems is very important.

The main purpose of this study is to explore the adsorption characteristics and performance of the as-synthesized and template-containing MCM-41 adsorbents for the removal of SDBS from aqueous solutions. We used ethanolic ammonium nitrate solution for expelling out parts of the template molecules that were used for synthesizing MCM-41. Also, the influences of determinant factors including pH, contact time, initial concentration of the surfactant, and adsorbent dose on the adsorption efficiency were performed on our best template-containing MCM-41. The kinetics, isotherms, and thermodynamics of the adsorption and regeneration of the adsorbents have also been studied.

2. Materials and methods

2.1. Synthesize and preparation of adsorbents

The silica mesoporous MCM-41 was synthesized by a room temperature procedure [41]. First, 2.9 g ethylamine was added to 45 mL distilled water and was mixed for 10 min at room temperature. Then 1.48 g CTAB (Merck, Germany, 1.02342) as structure-directing template was gradually added to the mixing solution and the stirring was continued for about 30 min. In the next step, 4.57 mL tetraethylorthosilicate (Merck, Germany, 800658) was added dropwise to the solution. The pH of the solution was about 12. By slow addition of HCl (1 mol L^{-1}) pH was decreased to 8.5 to observe that the white precipitate is forming. The slow mixing was continued for 2 h. Then, the formed precipitate was separated by centrifuging. The isolated solid was washed with warm distilled water several times. The collected sample was dried at 45°C for 12 h. This sample was named as MCM-41-AS.

Ion exchange technique was used to remove different amounts of the template from MCM-41-AS. For this purpose, 0.5 g of MCM-41-AS was dispersed in 75 mL of 60°C ethanolic ammonium nitrate (0.01 mol L^{-1}). The mixture was stirred for 15 min then the solid was recovered by centrifuging, washed with cold ethanol, and dried at 45°C overnight. This sample was designated as MCM-41-E1. This procedure was repeated for the second and third times. The samples obtained from these two steps were named as MCM-41-E2 and MCM-41-E3, respectively. Supposing the complete removal of template, 0.5 g of MCM-41-AS was heated at 550°C for 10 h under a programmed rising temperature (1°C min^{-1}). This sample is named as MCM-41-C [30].

2.2. Characterization

A Panalytical Xpert PRO (The Netherlands) X-ray diffraction instrument was used to give low angle XRD pattern of the adsorbents within a range of 2θ of 1°–10°. The textural parameters for the adsorbents were obtained using porosity analyzer PHS-1020 (PHSCHINA, China). A Nickolet FTIR instrument, Thermo Fisher Scientific (USA), was used to record the FTIR spectra of the bare and modified MCM-41 samples. Thermo-gravimetric analysis (TGA) was performed by a SDT Q600 V20.9 Build 20 instrument Artisan Technology Group (USA), the range of 25°–600°C and with a 10 min^{-1} temperature ramp were used. Transmission electron microscopy (TEM) was performed using a Philips CM120 instrument (The Netherlands) with an accelerating voltage of 100 kV.

2.3. Determination of SDBS in aqueous solutions

A stock standard solution of SDBS (purchased from Sigma Aldrich) was prepared by dissolving an accurately weighed amount of SDBS in distilled water to yield a concentration of 1,000 mg L^{-1} of the surfactant. Various concentrations of SDBS (1.0–1.5 mg L^{-1}) were prepared by subsequent dilution of the stock solution. A common and sensitive spectrophotometric method based on the formation of ion-pair between SDBS and methylene blue (MB) in an aqueous medium was used for the measurement of SDBS. In the practical procedure, extraction of the ion pair (MB$^+$DBS$^-$) by chloroform and measuring of the absorbance of the extract at 654 nm (as λ_{max}) was used for the determination of SDBS [42]. A Perkin Elmer lambda25 spectrophotometer was employed for the spectrophotometric determination of SDBS. The calibration curve was prepared as absorbance vs. SDBS concentrations.

2.4. Adsorption experiments

Batch adsorption experiments were performed by dispersing of a known weight of the adsorbents in a 100 mL solution of SDBS with a known concentration. This solution was stirred at a known pH and contact time to reach equilibrium. In order to acquire maximum adsorption, factors such as pH, contact time, the initial concentration of SDBS, and adsorbent dose were optimized. When the adsorption process reached equilibrium, a part of the supernatant solution was removed and centrifuged. The concentration of SDBS in the centrifuged solution was measured as mentioned in section 2.3 (Determination of SDBS in aqueous solutions).

The adsorption capacity (q_e) and removal percentage of surfactant from aqueous solutions was calculated from the difference between the initial and final concentrations of SDBS in the solutions as indicated below:

$$q_e = \frac{C_0 - C_e}{w} \times V \tag{1}$$

$$\%\text{Removal} = \left(1 - \frac{C_e}{C_0}\right) \times 100 \tag{2}$$

In these equations, C_0 and C_e (mg L^{-1}) are concentrations of SDBS at the initial and the equilibrium state, respectively; w (g) is the weight of adsorbent; V (L) is the volume of the suspension; and q_e (mg g^{-1}) is the amount of SDBS adsorbed on the adsorbent.

3. Results and discussion

3.1. Characterization of the adsorbents

3.1.1. Structural analysis

The prepared samples were characterized through low angle XRD measurement. As illustrated in Fig. 1 the
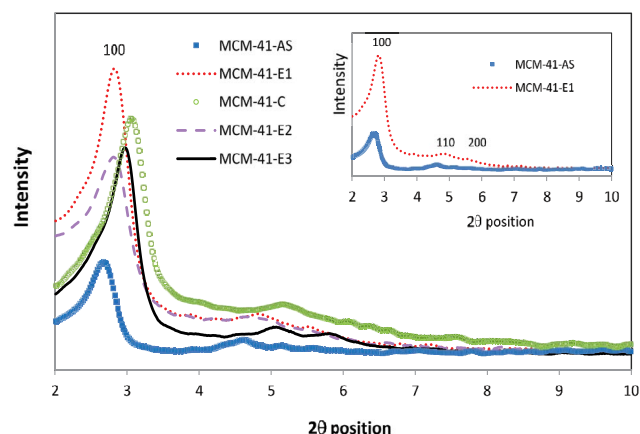
Fig. 1. Low-angle XRD patterns of adsorbents.

XRD patterns of all samples show a strong peak about 2° known as Miller plane 100 which confirms the MCM-41 hexagonal arranged channels [31]. Generally, by decreasing the template content, 2θ values related to the main peak (the most intense one which appears at 2.67° for MCM-41-AS) is shifted to higher values and d_{100} spacing is decreased [43]. Numerical values of 2θ and d_{100} related to the main peak are given in Table 2 for all the samples.

3.1.2. Textural analysis

The textural data in Table 2 imply that the specific surface area are increased by removal of CTAB from the channels of MCM-41. The table shows that MCM-41-C (thermally-treated sample) has the highest value (1,238 m² g⁻¹) while the MCM-AS with the maximum template content, has the lowest value (54.5 m² g⁻¹).

3.1.3. Spectral analysis

FTIR measurement was performed to verify the cationic template diminution in the mesoporous adsorbents structures. A pressed disc of the dispersed sample in KBr powder with a 1:100 ratio was prepared and then the IR spectrum was recorded. According to Fig. 2 two strong peaks around 2,900 cm⁻¹ (2,920 and 2,851 cm⁻¹) and the medium peak about 1,480 cm⁻¹ are assigned to symmetric and asymmetric stretching mode of –CH₂ group and bending of –CN group of CTAB in MCM-41-AS, respectively. The reduction of the intensity of these peaks is correlated to decreasing of CTAB content in the modified samples.

The peaks are very weak in MCM-41-E3 and it would disappear completely in the MCM-41-C due to complete degradation and escaping of the template molecules from the pores.

3.1.4. Thermal analysis

Three distinct regions of weight loss are recognizable in the thermogram of MCM-41-AS (Fig. 3). The first region of weight loss (50°C–150°C) is attributed to the loss of water molecules that were adsorbed physically on the surface of the mesoporous. The weight loss between 150°C and 350°C (the second region) is due to template desorption and decomposition. Finally, the third region (350°C–550°C) is related to the exclusion of water formed due to condensation of adjacent silanol groups. According to the recorded TGA data, the values of the weight losses were calculated for all the adsorbents and are shown in Table 3. It is observed from the thermograms (Fig. 3) that the amount of the template persisted into MCM-41 after the exchange treatment become lower from MCM-41-E1 to MCM-41-E3. These reductive weight losses are quantitatively 37.51%, 14.12%, and 6.59% for MCM-41-E1, MCM-41-E2, and MCM-41-E3, respectively (Table 3).

Our further studies for evaluating the adsorption efficiency of the as-synthesized, the calcined, and all the modified samples showed that MCM-41-E1 is the most effective adsorbent for SDBS. Therefore, the complementary characterization, optimizing the adsorption conditions, and thermodynamic studies were performed solely on MCM-41-E1.

3.1.5. Particle analysis

Fig. 4 illustrates TEM micrographs of MCM-41-E1 at two enlargements. In Fig. 4, partial filling of the channel of MCM-41-E1 could be observed. The darker spots indicate the presence of the template molecules remained in the channels of MCM-41-E1. The different intensity of the darkness for the observed particles may imply that the amounts of the persisted template molecules in the channels are a little different from each other. However, our TGA studies above gives the amount of the persisted template as an average value.

3.2. Adsorption studies

According to the TGA data, MCM-41-E1 has lots of persisted template. These are the surfactant molecules that are confined as micelles in the channels of MCM-41 following the

Table 2
Structural and textural data of adsorbents

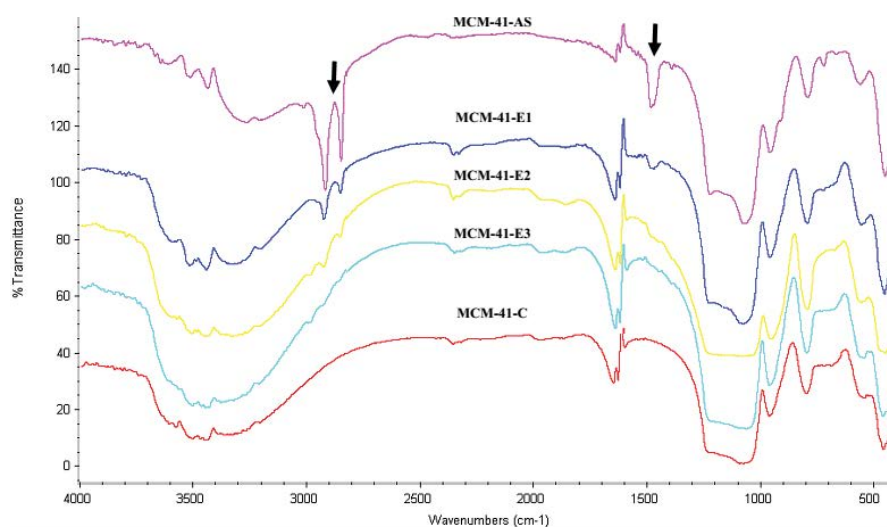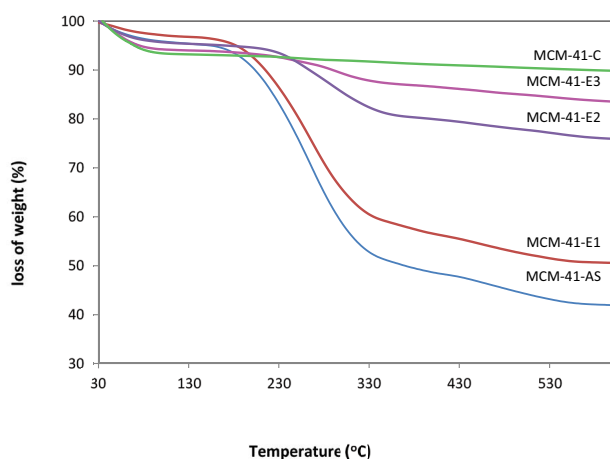| Parameters	MCM-41-AS	MCM-41-E1	MCM-41-E2	MCM-41-E3	MCM-41-C
2θ (degree)	2.67	2.79	2.91	2.97	3.05
XRD d_{100} spacing (Å)	33.06	31.64	30.34	29.72	28.94
Specific surface area (m² g⁻¹)	54.5	482.3	919.1	1,112.1	1,238
Pore volume (cm³ g⁻¹)	0.238	0.597	0.811	0.945	0.528
Average pore diameter (nm)	1.26	1.64	1.71	1.71	1.37

Fig. 2. FTIR spectra of adsorbents.

Fig. 3. TGA thermograms for adsorbents.

ion exchange treatment. MCM-41-E1 contains less micelles than MCM-41-AS because of expelling out some of the surfactant molecules via ion exchange. We found MCM-41-E1 as the most efficient adsorbent for SDBS and we studied it further for finding out the optimal conditions which affect the adsorption capacity.

3.2.1. Effect of pH

The pH of the solution affects several interactional properties in adsorbate–adsorbent scheme including the surface charge of the adsorbent. Fig. 5 illustrates the effect of initial pH on the adsorption capacity of SDBS onto MCM-41-E1. The adsorption capacity is significantly dependent on pH of the medium. The capacity decreases when pH of the system changes from 5.1 to higher values. Therefore, acidic range was the best region for the adsorption studies. The observed variation in the adsorption capacity with respect to the pH of the initial solution can be clarified based on the structure of SDBS molecule and point of zero charge of adsorbent. The point of zero charge for

MCM-41-E1 is estimated to be about 5.0 [30]. Above this pH, especially at high pH, the adsorbent gets a negative charge. Therefore, the electrostatic repulsion between DBS⁻ anions and negative surface of the mesoporous causes a decrease in the adsorption capacity.

3.2.2. Effect of contact time and initial concentrations

Contact time affects the adsorption capacity of MCM-41-E1 at different initial SDBS concentrations. Three different initial concentrations of 200, 300, and 400 mg L⁻¹ were used. SDBS adsorption was rapid in the first 20 min and then progressed at a slower rate and finally reached equilibrium after 30 min. The adsorption is higher in the beginning because of the greater number of sites available for the adsorption of SDBS. This is a common feature in heterogeneous reactions taking place between the adsorbing species in liquid phase and adsorbent sites of the solid. From Fig. 6, it is evident that the adsorption increases clearly with initial concentration of SDBS [44].

3.2.3. Effect of adsorbent weight

Adsorption performance of SDBS solutions containing various amounts of MCM-41-E1 (10, 20, 35, 50, 70, 100, 150, and 200 mg) were studied at optimum conditions. According to Fig. 7, adsorption capacity (q_e) decreases when adsorbent dose increases [44]. The decrease of the adsorbed SDBS per unit weight of adsorbent was most probably due to the concentration gradient between the adsorbate and adsorbent described by Nandi et al. [45]. The decreasing in the effective adsorption with increasing adsorbent dose may be due to the formation of aggregates [46]. In contrary, SDBS removal percentage obviously increases with respect to increasing adsorbents particles until it reaches a maximum value (94%) at 100 mg (0.1 g) and then remains almost constant [22]. When the weight of adsorbent increases, the available sites on the adsorbent are in higher amounts and provides more active sites to adsorb SDBS which results in increasing adsorption [47].

Table 3
TGA data for adsorbents

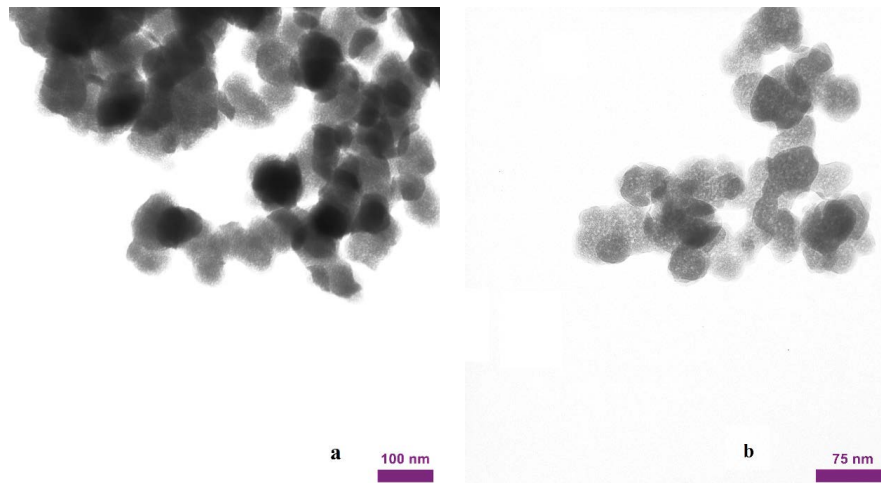| Thermal region (°C)	Weight loss (%)				
	MCM-41-AS	MCM-41-E1	MCM-41-E2	MCM-41-E3	MCM-41-C
50–150	2.93	2.22	2.69	3.60	4.20
150–350	43.26	37.51	14.12	6.59	1.56
350–550	8.57	8.03	4.40	3.15	1.41

Fig. 4 Transmission electron microscopy of MCM-41-E1 at two enlargements; (a) 100 nm and (b) 75 nm.
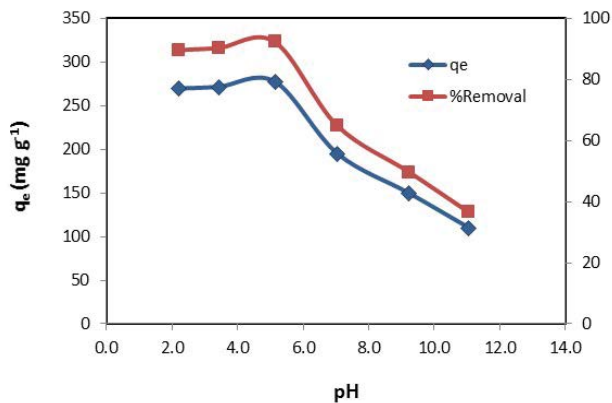

Fig. 5. Influence of pH on the adsorption of SDBS. Volume and concentration of SDBS: 100 mL and 300 mg L^{-1}, respectively. Weight of MCM-41-E1: 0.1 g at room temperature.

Fig. 6. Adsorption capacity of MCM-41-E1 for SDBS with regard to contact time. Three different 200, 300, and 400 mg L^{-1} initial concentrations of SDBS were used. Weight of MCM-41-E1: 0.1 g and pH = 5.0.

3.2.4. Adsorption performance, proposed mechanism, and isotherms

The equilibrium adsorption of SDBS solutions (concentration range: 100–1,000 mg L^{-1}) onto the prepared samples was studied at optimum conditions. Fig. 8 shows variation of q_e with the initial concentration of SDBS. Maximum performance belongs to MCM-41-E1. The presence of CTAB within the channels of template-containing samples changes the surface chemistry of MCM-41. In MCM-41-AS, hydrophobic interactions between hydrocarbon tails of
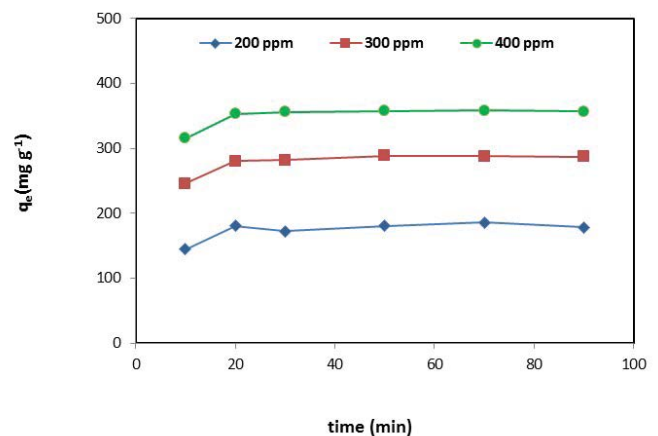
SDBS and CTAB in monolayers of surfactants (hemimicelles) are responsible for adsorption. But in MCM-41-E1, combination of hydrophobic and electrostatic interactions are driving forces for SDBS adsorption [30]. As mentioned previously, in MCM-41-E1 a free space was created by expelling out part of the template. The formation of bilayers of CTAB (admicelles) which cause enrichment of positive charge on the surface of mesoporous are due to the template removal. According to this new condition, SDBS molecules which
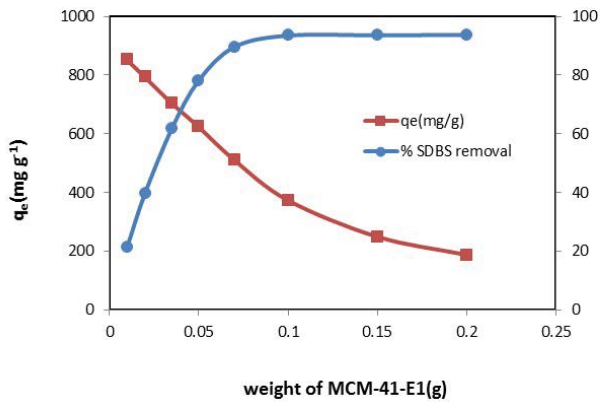
Fig. 7. Effect of MCM-41-E1 weight on its adsorption efficiency. 100 mL of SDBS 400 mg L^{-1} at pH 5.0 and contact time 30 min.
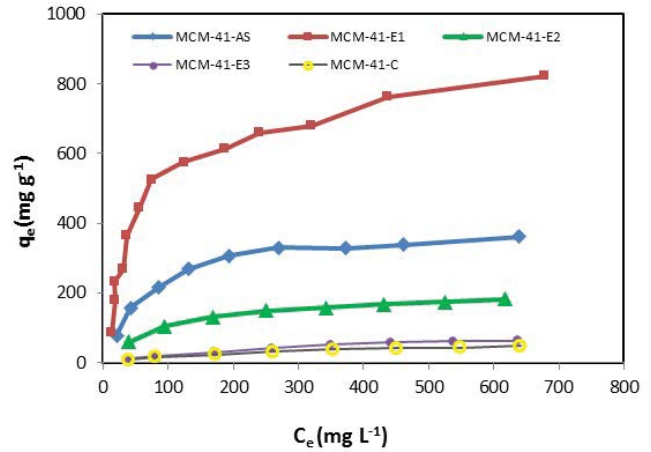

Fig. 8. Adsorption isotherms of prepared adsorbents at room temperature at optimal conditions (pH 5.0, contact time 30 min, and adsorbent weight 0.1 g).

are solubilized into the hydrophobic space of admicelles found further interactions (electrostatic types) between DBS$^-$ and the template positive species (CTMA$^+$).

Figs. 9a and b illustrate the proposed interactions between SDBS and CTMA$^+$ in monolayers (hydrophobic interaction) and bilayers (hydrophobic and electrostatic interaction) formed inside of the channels of MCM-41-E1, respectively [30]. In MCM-41-E2, it seems that the electrostatic type interaction between SDBS and MCM-41-E2 is not likely because the expelling out of most of the template species does not lead to formation of bilayers and therefore the formation of additional positive charges based on the admicelles is improbable. In this situation, the interaction is restricted to hydrophobic interactions only, and (hemimicelles are dominant). Finally, MCM-41-E3 and MCM-41-C, both show little adsorption tendency toward SDBS. These later mesoporous adsorbents contain very low amount of template (based on TGA results) and therefore the adsorption of SDBS due to the template would be low.

The fitness of obtained adsorption data for the three types of isotherm models including Langmuir, Freundlich, and Temkin were tested. The Langmuir model assumes that there are a certain number of active sites that are homogenously dispersed over the surface of the adsorbent. There is no interaction between the adsorbed molecule. The experimental data are conventionally fitted to the linear form of the Langmuir equation as below:

$$\frac{C_e}{q_e} = \frac{C_e}{q_m} + \frac{1}{K_L \cdot q_m} \quad (3)$$

where q_e (mg g^{-1}) is the amount of SDBS adsorbed, C_e (mg L^{-1}) is the equilibrium concentration of the adsorbate, q_m (mg g^{-1}) and K_L (L mg^{-1}), are Langmuir constants related to the maximum adsorption capacity and energy of adsorption, respectively. A plot of C_e/q_e vs. C_e would result in a straight line with a slope of $1/q_m$ and intercept of $1/K_L \cdot q_m$ as can be seen in Fig. 10a.

The affinity between the SDBS and mesoporous adsorbents can be calculated by the dimensionless separation factor, R_L which is determined by the following equation:
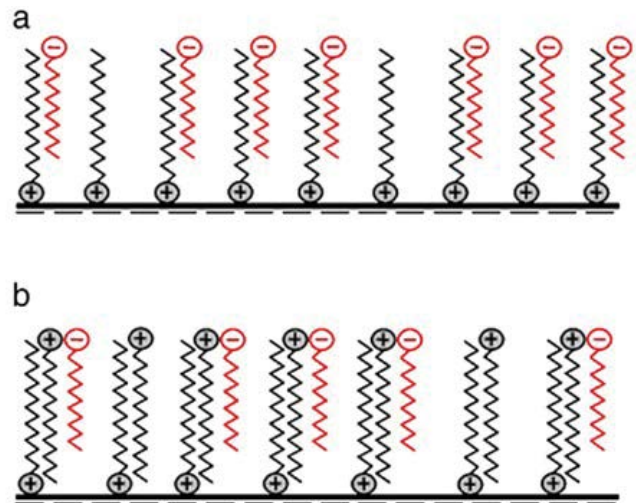
Fig. 9. Illustrations of the proposed mechanism based on the interactions between SDBS and CTMA$^+$ inside of the channels of MCM-41-E1. (a) Hydrophobic interaction in monolayers and (b) hydrophobic and electrostatic interactions in bilayers.

$$R_L = \frac{1}{\left(1 + K_L \cdot C_0\right)} \quad (4)$$

The relation between R_L and C_0 for the adsorption of SDBS onto all the samples is shown in Fig. 10b. The calculated values of R_L which located between 0 and 1 ($0 < R_L > 1$) indicate that the adsorption of SDBS on the adsorbents is favorable and it is more favorable at higher initial concentrations of SDBS.

Freundlich isotherm model considers a heterogeneous surface containing irregular available adsorption sites with a different energy. The model is described by the following linear relation:

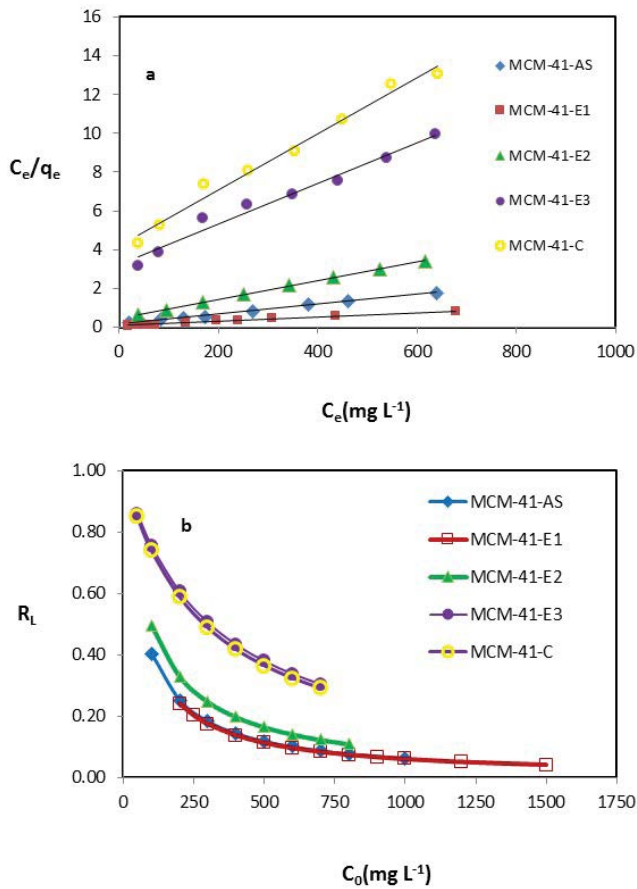$$\log q_e = \log K_F + \frac{1}{n} \log C_e \quad (5)$$

Fig. 10. Langmuir isotherm plots for adsorption of SDBS on prepared adsorbents at optimal conditions (pH 5.0, contact time 30 min, and adsorbent weight 0.1 g) (a) and plots of R_L vs. C_0 (b).
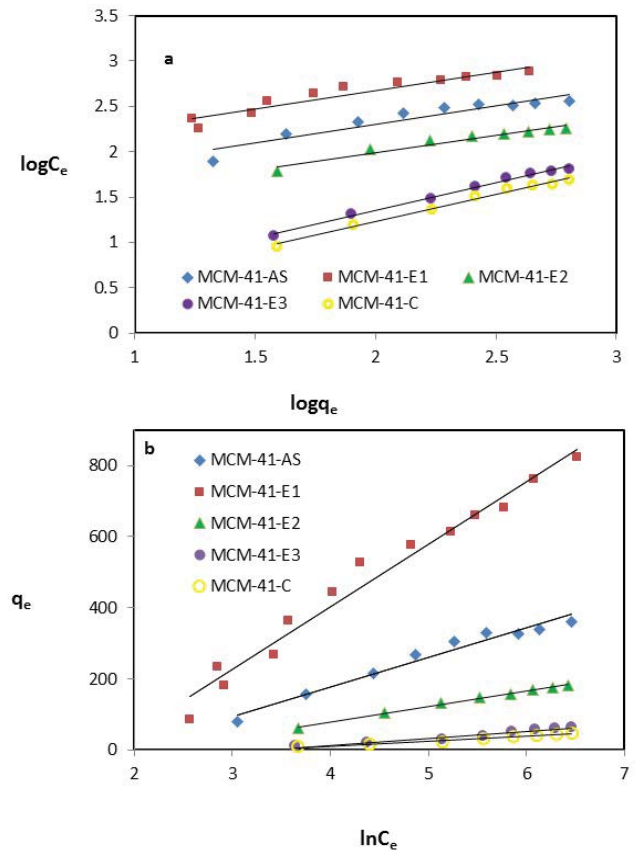

Fig. 11. Freundlich (a) and Temkin (b) isotherm plots of adsorption of SDBS on prepared samples at optimal conditions (pH 5.0, contact time 30 min, and adsorbent weight 0.1 g).

where q_e is the amount of adsorbed (mg g^{-1}), C_e is the equilibrium concentration of adsorbate (mg L^{-1}). The K_F and n (mg$^{(1-1/n)}$ g^{-1} L$^{1/n}$) are constant and are related to adsorption capacity and desorption intensity, respectively. Fig. 11a shows a plot of $\log q_e$ vs. $\log C_e$ in which Freundlich constants for the adsorption systems can be calculated from the intercept and slope.

In the Temkin model, it is assumed that the heat of adsorption (ΔH°_{ads}) of all molecules decreases linearly with increasing coverage layer of adsorbate. The adsorption is considered by a uniform distribution of binding energies. Temkin isotherm is described by the following linear equation:

$$q_e = B \ln A_T + B \ln C_e \tag{6}$$

$$B = \frac{RT}{b} \tag{7}$$

where q_e is the amount of adsorbate (mg g^{-1}) and C_e is the equilibrium concentration of adsorbate (mg L^{-1}). The A_T is Temkin binding constant resembling the maximum binding energy (L g^{-1}) and B is a constant related to the heat of sorption (J mol^{-1}) which is associate to b Temkin isotherm

constant. The constants A_T and B are found from the intercept and slope of the plot q_e vs. $\ln C_e$, respectively, as shown in Fig. 11b.

The parameters and correlation coefficients (R^2) obtained from linear equations of all the three isotherm models are given in Table 4. However, it seems that Freundlich isotherm is more appropriate to describe the adsorption of the SDBS onto MCM-41-E3 and MCM-41-C. This commonly suggests a heterogeneous distribution of sites on the surface of these adsorbents [30].

According to adsorption isotherm data MCM-41-E1 is more favorite adsorbent for removal of SDBS. Therefore, kinetics and thermodynamic studies of adsorption of SDBS onto this mesoporous was studied.

3.2.5. Adsorption kinetics

Kinetic studies are frequently essential to provide information about the mechanism of the adsorption and predict whether the adsorbent/adsorbate interaction is physisorption or chemisorption. Different reaction models such as pseudo-first-order, pseudo-second-order, and intra-particle diffusion were applied to study adsorption rate of SDBS (at different concentration of 200, 300, and 400 mg L^{-1}) onto MCM-41-E1. The Lagergren's first-order-rate equation is used at first step:

Table 4
Isotherm parameters for SDBS adsorption onto prepared adsorbents

Isotherm		Adsorbents				
		MCM-41-AS	MCM-41-E1	MCM-41-E2	MCM-41-E3	MCM-41-C
	R^2	0.9942	0.9945	0.9990	0.9774	0.9847
Langmuir	q_m (mg g^{-1})	398.3	874.7	203.9	95.1	69.0
	K_L (L mg^{-1})	0.0145	0.0158	0.0102	0.0033	0.0034
	R_L	$0.40 < R_L > 0.06$	$0.39 < R_L > 0.041$	$0.49 < R_L > 0.11$	$0.86 < R_L > 0.30$	$0.85 < R_L > 0.29$
	R^2	0.8864	0.9026	0.9506	0.9930	0.9903
Freundlich	$1/n$	0.412	0.402	0.379	0.606	0.600
	K_F (mg$^{(1-1/n)}$ g^{-1} L$^{1/n}$)	30.28	74.85	17.17	1.37	1.061
	R^2	0.9662	0.9737	0.9646	0.9650	0.9744
Temkin	A_T (L g^{-1})	7.5×10^{-4}	0.020	1.07×10^{-6}	6.28×10^{-14}	1.25×10^{-18}
	B (J mol^{-1})	82.74	175.5	43.30	19.59	14.44

$$\ln\left(q_e - q_t\right) = \ln q_e - k_1 \times t \tag{8}$$

In this linear equation, q_e (mg g^{-1}) is the adsorption amount at equilibrium, t (min) is the contact time, and k_1 (min^{-1}) is the rate constant. As shown in Fig. 12a, they are obtained from the linear plot of $\ln(q_e - q_t)$ vs. t which makes possible the calculation of q_e and k_1 from the slope and intercept of the line.

The kinetics of a second-order-rate expression could be given as a linearized form as below:

$$\frac{t}{q_t} = \frac{1}{k_2 q_e^2} + \frac{1}{q_e} \times t \tag{9}$$

where q_e (mg g^{-1}) and q_t (mg g^{-1}) are the adsorption amount at equilibrium and time t, respectively, t (min) is the contact time, and k_2 (g mg^{-1} min^{-1}) is the rate constant for a second-order-rate of adsorption. The q_e and k_2 are calculated from the slope and intercept of the plot of t/q_t against t, respectively. Fig. 12b illustrates the straight line plots of t/q_t vs. t for the adsorption of SDBS onto MCM-41-E1. Table 5 gives all the values of k_1, k_2, and q_e, and also their corresponding regression coefficient values (R^2). For the pseudo-second-order kinetics values of R^2 are close to unity suggesting that the adsorption of SDBS onto MCM-41-E1 is well-described by a pseudo-second-order model.

The effect of temperature on the adsorption kinetics of SDBS onto MCM-41-E1 was also studied. Three different temperatures of 25°C, 35°C, and 45°C were applied. According to the data given in Table 5, the rate constants and q_e values are slightly increased with temperature raises. This can be expected for the adsorption systems based on physisorption. When temperature raises the solution viscosity decreases and subsequently rate of the diffusion of the molecules across the adsorbent layers increase. To describe the variation of the rate of a chemical reaction with temperature Eyring equation could be used. Fig. 13 shows the Eyring plot assuming a second-order-rate constants. The activation parameters can be calculated by Eyring equation as below:

$$\ln\left(\frac{k}{T}\right) = \frac{-\Delta H^{\#}}{RT} + \ln\frac{k_B}{h} + \frac{\Delta S^{\#}}{R} \tag{10}$$

where k (or k_2) is the pseudo-second-order rate constant of adsorption, k_B and h are the Boltzmann and the Plank constants, respectively; R is the universal gas constant, T is temperature, $\Delta H^{\#}$ is enthalpy, and $\Delta S^{\#}$ is entropy. The values for $\Delta H^{\#}$ and $\Delta S^{\#}$ can be determined from kinetic data obtained from a $\ln k_2/T$ vs. $1/T$ plot. The equation is a straight line with negative slope, $\dfrac{-\Delta H^{\#}}{R}$ and an intercept, $\dfrac{\Delta S^{\#}}{R} + \ln\dfrac{k_B}{h}$.

3.2.6. Thermodynamic studies

The adsorption of SDBS onto MCM-41-E1 could be studied further. To observe the effect of temperature, the adsorption studies of SDBS (concentrations from 200 to 1,000 mg L^{-1}) onto MCM-41-E1 were performed at three different temperatures: 25°C, 35°C, and 45°C. Thermodynamic parameters including enthalpy (ΔH_{ads}°), the Gibbs free energy change (ΔG_{ads}°), and entropy change (ΔS_{ads}°) were estimated by the following equations:

$$K_0 = \frac{C_{e,solid}}{C_e} \tag{11}$$

$$\Delta G_{ads}^{\circ} = -RT \ln K_0 \tag{12}$$

$$\ln K_0 = \frac{\Delta S_{ads}^{\circ}}{R} - \frac{\Delta H_{ads}^{\circ}}{RT} \tag{13}$$

where K_0 is the distribution coefficient, $C_{e,solid}$ and C_e (mL g^{-1}) are equilibrium concentration of adsorbate in solid (adsorbed) and liquid, respectively, ΔG_{ads}° is standard Gibbs free energy (kJ mol^{-1}), ΔS_{ads}° is standard entropy (J mol^{-1} K^{-1}), ΔH_{ads}° is standard enthalpy (kJ mol^{-1}), T is the absolute temperature (K), and R is the gas constant (8.314 J mol^{-1} K^{-1}). A plot of $\ln K_0$ vs. $1/T$ gives straight line in which its slope and intercepts would give enthalpy and entropy changes, respectively (Fig. 14). According to Table 6, K_0 values increased when the

temperature increased. Therefore, the adsorption is facilitated and becomes more favorable at higher temperatures.

Thermodynamic parameters (ΔH°_{ads}, ΔS°_{ads}, and ΔG°_{ads}) are also given in Table 6. The positive values of enthalpy change (ΔH°_{ads}) calculated for the adsorption systems confirm the endothermic nature of the adsorption process and the positive values of ΔS°_{ads} indicated the increased randomness of the adsorbate molecules on the solid surfaces than in the solution [48]. Entropy is favorable, so the adsorption process is governed by entropic rather than enthalpy changes. On the other hand, the negative free energy values ΔG°_{ads} of the adsorption process refers that it's

spontaneous. The value of ΔG°_{ads} increases with temperature, implying to more favorable reaction at higher temperature.

3.3. Regeneration of adsorbent

From dependency of the adsorption capacity of MCM-41-E1 to pH it is found that by increasing the pH, desorption
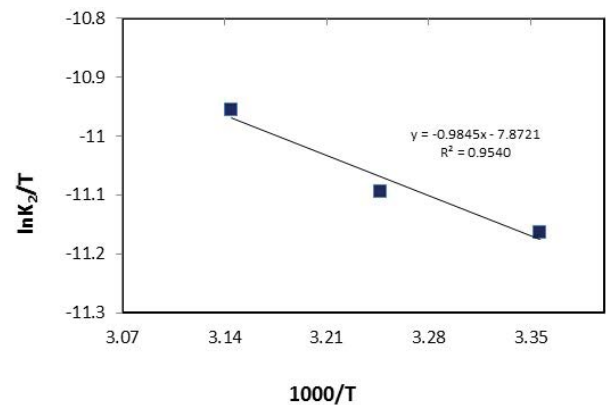
Fig. 13. Eyring plot of pseudo-second-order kinetic for the adsorption of 100 mL SDBS 300 mg L^{-1} onto MCM-41-E1 (pH 5.0, contact time 30 min, and adsorbent weight 0.1 g).
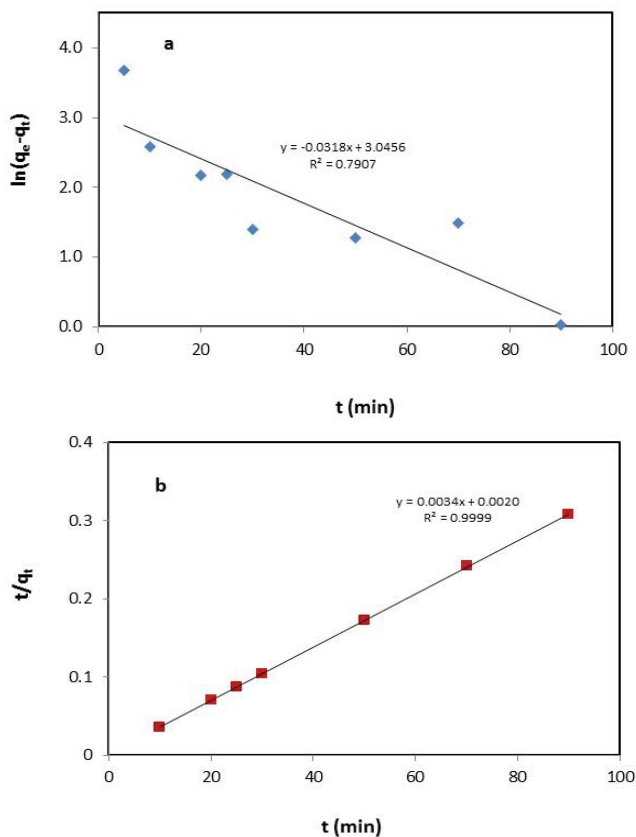

Fig. 12. Pseudo-first-order (a) and pseudo-second-order (b) kinetic plots for the adsorption of 100 mL of SDBS 300 mg L^{-1} onto MCM-41-E1 (pH 5.0, contact time 30 min, and adsorbent weight 0.1 g).
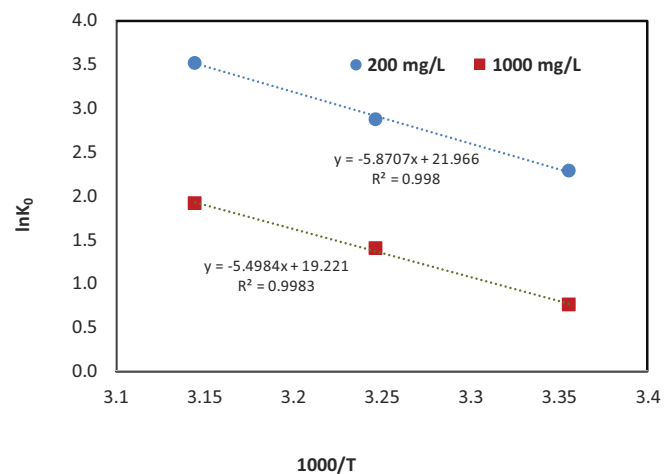
Fig. 14. Plots of $\ln K_0$ vs. $1/T$ for the adsorption of various concentrations (200 and 1,000 mg L^{-1}) of SDBS onto MCM-41-E1 at optimum conditions.

Table 5
Kinetic parameters and effect of temperature for adsorption of 100 mL SDBS 300 mg L^{-1} onto MCM-41-E1 (pH 5.0, contact time 30 min, and adsorbent weight 0.1 g)

| Temperature (K) | Pseudo-second-order parameters | | | Pseudo-first-order |
	k_2 (g mg min^{-1})	q_e (mg g^{-1})	R^2	R^2
298	4.4×10^{-3}	290.2	0.9998	0.6152
308	5.0×10^{-3}	291.4	0.9999	0.7698
318	5.7×10^{-3}	293.5	0.9999	0.7907
Activation parameters		ΔH° (kJ mol^{-1})	7.84	ΔS° (J mol^{-1} K^{-1}) –263.78

might be occurred. On this basis, by using a 0.1 mol L^{-1} sodium hydroxide and changing the pH of the treating aqueous media to highly alkaline, the used MCM-41-E1 was treated for 30 min. The adsorbed SDBS were desorbed upon this treatment. Then the adsorbent was separated from the solution and was recovered by centrifugation. Finally, the regenerated adsorbent was dried in 45°C overnight. The recapture adsorbent named R_1 was used again for the next batch adsorption system (100 mL SDBS 300 mg L^{-1}) at optimum conditions. The performance of R_1 was 96% of fresh adsorbent. The recycling processes was repeated. The adsorbent (R_2) preserve 84% of its fresh efficacy. The result implies good reusability of the adsorbent and its ability to removal of SDBS even after three cycles used. The results are shown in Fig. 15.

3.4. Real samples: removal of SDBS from wastewaters

Wastewater samples from a known manufacturing factory of detergents (dishwashing and laundry) and an industrial city were collected and were studied. The samples first were filtered then concentration of SDBS was determined by the method previously described in this work. The SDBS concentrations were 715 and 39.4 mg L^{-1} for the waste of the factory and the industrial city, respectively. Batch adsorption tests were performed by treating 100 mL of water samples containing 0.1 g MCM-41-E1 at our optimum conditions. Then, concentrations of SDBS in the supernatants were measured and the results confirmed

the mesoporous adsorbents efficiency for removal of SDBS from waste (94.0% and 86.2% removal for the factory and industrial city wastes, respectively).

3.5. Comparison with other adsorbents

Providing a clear judgment for readers, the adsorption capacity of SDBS onto MCM-41-E1 was compared to some adsorbents recorded in literatures. According to Table 7, the adsorption capacity of MCM-41-E1 is greater than those previously reported, confirming its high efficiency for removal of SDBS from contaminated waters.
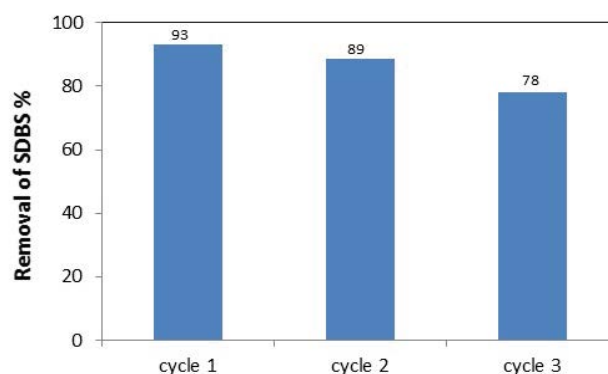

Fig. 15. Performance of regenerated adsorbent.

Table 6
Thermodynamics parameters for adsorption of SDBS onto MCM-41-E1

C_0 (mg L^{-1})	K_0			ΔG°_{ads} (kJ mol^{-1})			ΔH°_{ads} (kJ mol^{-1})	ΔS°_{ads} (J mol^{-1} K^{-1})
	298 K	308 K	318 K	298 K	308 K	318 K		
200	9.79	17.71	33.84	−5.65	−7.12	−8.73	48.81	182.63
300	8.74	27.71	45.80	−5.37	−8.23	−9.48	65.49	238.60
500	7.97	17.80	20.39	−5.14	−7.13	−7.47	37.27	143.18
600	7.13	14.81	15.53	−4.87	−6.68	−6.80	30.95	121.07
700	4.64	9.22	11.55	−3.80	−5.50	−6.06	36.09	134.44
800	3.28	6.78	9.00	−2.94	−4.74	−5.44	39.93	144.43
900	2.76	5.35	7.96	−2.51	−4.16	−5.14	41.86	149.22
1,000	2.13	4.04	6.79	−1.87	−3.46	−4.75	45.71	159.80

Table 7
Comparison of SDBS adsorption capacities by other adsorbents

Adsorbent	q_m (mg g^{-1})	Reference
Styrene (St)-based crosslinked resin beads (HP20)	57.9	[21]
Methyl methacrylate (MMA)-based crosslinked resin beads (HP2MGL)	15.5	
Montmorillonite	140	[25]
High area activated carbon cloth	344	[20]
Styrene-divinyl-benzene polymer resin	864	[49]
Acrylic ester polymer resin	592	
Alumina	19.8	[50]
MCM-41-E1	874	Present study

4. Conclusion

The adsorption of SDBS onto MCM-41 and its modified samples as adsorbents were investigated under optimum conditions. The modified MCM-41 samples contained less template inside the structure in comparison with the as-synthesized one. The kinetic of the adsorption were fully studied. Different models of adsorption isotherm and various kinetic models were used for fitness of the experimental data. The results show that a modified MCM-41 with a certain range of template shows the most efficient adsorbent for the removal of SDBS. The adsorbent was successfully regenerated and its efficiency remains significant even after three cycles of use. The adsorbent has considerable potential for the removal of SDBS from industrial wastewaters.

Acknowledgments

Symbols

q_e	—	Adsorption capacity, mg g^{-1}
C_0 and C_e	—	Concentrations of adsorbate at the initial and the equilibrium state, mg L^{-1}
w	—	Weight of adsorbent, g
V	—	Volume of the suspension, L
q_m	—	Maximum adsorption capacity, mg g^{-1}
K_L	—	Energy of adsorption, L mg^{-1}
R_L	—	Separation factor
K_F and n	—	Freundlich constant related to adsorption capacity, mg$^{(1-1/n)}$ g^{-1} L$^{1/n}$ and desorption intensity
B	—	Constant related to the heat of sorption, J mol^{-1}
A_T	—	Temkin binding constant resembling the maximum binding energy, L g^{-1}
b	—	Temkin isotherm constant
k_1	—	Pseudo-first-order rate constant, min^{-1}
t	—	Contact time, min
k_2	—	Pseudo-second rate constant, g mg^{-1} min^{-1}
q_t	—	Adsorption amount at time t, mg g^{-1}
k_B	—	Boltzmann constant
h	—	Plank constant
R	—	Universal gas constant, J mol^{-1} K^{-1}
T	—	Temperature, K
$\Delta H^{\#}$ and $\Delta S^{\#}$	—	Activation enthalpy, kJ mol^{-1} and entropy, J mol^{-1}
K_0	—	Distribution coefficient
$C_{e,\text{solid}}$	—	Equilibrium concentration of adsorbate in solid
$\Delta S^{\circ}_{\text{ads}}$, $\Delta H^{\circ}_{\text{ads}}$	—	Standard entropy, J mol^{-1} K^{-1} and standard enthalpy, kJ mol^{-1}
$\Delta G^{\circ}_{\text{ads}}$	—	Standard Gibbs free energy, kJ mol^{-1}

References

[1] G. Broze, Handbook of Detergents, Part A: Properties, CRC Press, New York, USA, 1999.

[2] P. Eichhorn, S. Rodriguez, W. Baumann, T. Knepper, Incomplete degradation of LABS in Brazilian surface waters and pursuit of their polar metabolites in drinking waters, Sci. Total Environ., 284 (2002) 123–134.

[3] S. Schulz, W. Dong, U. Groth, A.M. Cook, Enantiomeric degradation of 2-(4-sulfophenyl) butyrate via 4-sulfocatechol in *Delftia acidovorans* SPB1, Appl. Environ. Microbiol., 66 (2000) 1905–1910.

[4] T. Frömel, T.P. Knepper, Mass spectrometry as an indispensable tool for studies of biodegradation of surfactants, TrAC Trends Anal. Chem., 27 (2008) 1091–1106.

[5] K. Ikehata, M.G. El-Din, Degradation of recalcitrant surfactants in wastewater by ozonation and advanced oxidation processes: a review, Ozone Sci. Eng., 26 (2004) 327–343.

[6] G. Lissens, J. Pieters, M. Verhaege, L. Pinoy, W. Verstraete, Electrochemical degradation of surfactants by intermediates of water discharge at carbon-based electrodes, Electrochim. Acta, 48 (2003) 1655–1663.

[7] I. Kowalska, M. Kabsch-Korbutowicz, K. Majewska-Nowak, T. Winnicki, Separation of anionic surfactants on ultrafiltration membranes, Desalination, 162 (2004) 33–40.

[8] I. Kowalska, Surfactant removal from water solutions by means of ultrafiltration and ion-exchange, Desalination, 221 (2008) 351–357.

[9] S. Gupta, A. Pal, P.K. Ghosh, M. Bandyopadhyay, Performance of waste activated carbon as a low-cost adsorbent for the removal of anionic surfactant from aquatic environment, J. Environ. Sci. Health., Part A, 38 (2003) 381–397.

[10] B.-J. Shiau, J.H. Harwell, J.F. Scamehorn, Precipitation of mixtures of anionic and cationic surfactants: III. Effect of added nonionic surfactant, J. Colloid Interface Sci., 167 (1994) 332–345.

[11] T. Zhang, T. Oyama, S. Horikoshi, J. Zhao, N. Serpone, H. Hidaka, Photocatalytic decomposition of the sodium dodecylbenzene sulfonate surfactant in aqueous titania suspensions exposed to highly concentrated solar radiation and effects of additives, Appl. Catal., B, 42 (2003) 13–24.

[12] J. Kaleta, M. Elektorowicz, The removal of anionic surfactants from water in coagulation process, Environ. Technol., 34 (2013) 999–1005.

[13] M. Aboulhassan, S. Souabi, A. Yaacoubi, M. Baudu, Removal of surfactant from industrial wastewaters by coagulation flocculation process, Int. J. Environ. Sci. Technol., 3 (2006) 327–332.

[14] F. Karray, M. Mezghani, N. Mhiri, B. Djelassi, S. Sayadi, Scale-down studies of membrane bioreactor degrading anionic surfactants wastewater: isolation of new anionic-surfactant degrading bacteria, Int. Biodeterior. Biodegrad., 114 (2016) 14–23.

[15] M. Fedeila, Z. Hachaïchi-Sadouk, L.F. Bautista, R. Simarro, F. Nateche, Biodegradation of anionic surfactants by *Alcaligenes faecalis*, *Enterobacter cloacae* and *Serratia marcescens* strains isolated from industrial wastewater, Ecotoxicol. Environ. Saf., 163 (2018) 629–635.

[16] G.F. Murari, J.A. Penido, H.M. da Silva, B.E.L. Baêta, S.F. de Aquino, L.R. de Lemos, G.D. Rodrigues, A.B. Mageste, Use of aqueous two-phase PEG-salt systems for the removal of anionic surfactant from effluents, J. Environ. Manage., 198 (2017) 43–49.

[17] A. Vinu, T. Mori, K. Ariga, New families of mesoporous materials, Sci. Technol. Adv. Mater., 7 (2006) 753–771.

[18] Q. Gao, W. Chen, Y. Chen, D. Werner, G. Cornelissen, B. Xing, S. Tao, X. Wang, Surfactant removal with multiwalled carbon nanotubes, Water Res., 106 (2016) 531–538.

[19] H.M.A. El-Lateef, M.M.K. Ali, M.M. Saleh, Adsorption and removal of cationic and anionic surfactants using zero-valent iron nanoparticles, J. Mol. Liq., 268 (2018) 497–505.

[20] E. Ayranci, O. Duman, Removal of anionic surfactants from aqueous solutions by adsorption onto high area activated carbon cloth studied by *in situ* UV spectroscopy, J. Hazard. Mater., 148 (2007) 75–82.

[21] J. Kim, D. Kim, Y. Gwon, K.-W. Lee, T. Lee, Removal of sodium dodecylbenzenesulfonate by macroporous adsorbent resins, Materials, 11 (2018) 1324, doi: 10.3390/ma11081324.

[22] A. Adak, M. Bandyopadhyay, A. Pal, Removal of anionic surfactant from wastewater by alumina: a case study, Colloids Surf., A, 254 (2005) 165–171.

[23] A. Pal, S. Pan, S. Saha, Synergistically improved adsorption of anionic surfactant and crystal violet on chitosan hydrogel beads, Chem. Eng. J., 217 (2013) 426–434.

[24] G.Z. Kyzas, E.N. Peleka, E.A. Deliyanni, Nanocrystalline akaganeite as adsorbent for surfactant removal from aqueous solutions, Materials, 6 (2013) 184–197.

[25] K. Yang, L. Zhu, B. Xing, Sorption of sodium dodecylbenzene sulfonate by montmorillonite, Environ. Pollut., 145 (2007) 571–576.

[26] D.C. Rodríguez-Sarmiento, J.A. Pinzon-Bello, Adsorption of sodium dodecylbenzene sulfonate on organophilic bentonites, Appl. Clay Sci., 18 (2001) 173–181.

[27] S.R. Taffarel, J. Rubio, Adsorption of sodium dodecyl benzene sulfonate from aqueous solution using a modified natural zeolite with CTAB, Miner. Eng., 23 (2010) 771–779.

[28] N. Hemmati, A. Tabzar, M.H. Ghazanfari, Adsorption of sodium dodecyl benzene sulfonate onto carbonate rock: kinetics, equilibrium and mechanistic study, J. Dispersion Sci. Technol., 39 (2018) 687–699.

[29] H.M. Vale, T.F. McKenna, Adsorption of sodium dodecyl sulfate and sodium dodecyl benzenesulfonate on poly(vinyl chloride) latexes, Colloids Surf., A, 268 (2005) 68–72.

[30] A. Ariapad, M. Zanjanchi, M. Arvand, Efficient removal of anionic surfactant using partial template-containing MCM-41, Desalination, 284 (2012) 142–149.

[31] R.A. Melo, M.V. Giotto, J. Rocha, E.A. Urquieta-González, MCM-41 ordered mesoporous molecular sieves synthesis and characterization, Mater. Res., 2 (1999) 173–179.

[32] U. Ciesla, F. Schüth, Ordered mesoporous materials, Microporous Mesoporous Mater., 27 (1999) 131–149.

[33] R.I. Nooney, D. Thirunavukkarasu, Y. Chen, R. Josephs, A.E. Ostafin, Synthesis of nanoscale mesoporous silica spheres with controlled particle size, Chem. Mater., 14 (2002) 4721–4728.

[34] C. Coll, R. Martínez-Máñez, M.D. Marcos, F. Sancenón, J. Soto, R.K. Mahajan, Efficient removal of anionic surfactants using mesoporous functionalised hybrid materials, Eur. J. Inorg. Chem., 2009 (2009) 3770–3777.

[35] Y. Miyake, T. Yumoto, H. Kitamura, T. Sugimoto, Solubilization of organic compounds into as-synthesized spherical mesoporous silica, Phys. Chem. Chem. Phys., 4 (2002) 2680–2684.

[36] L. Borello, B. Onida, C. Barolo, K. Edler, C.O. Areán, E. Garrone, Accessibility of dye molecules embedded in surfactant-silica hybrid materials in both powder and film forms, Sens. Actuators, B, 100 (2004) 107–111.

[37] M. Ogawa, Photoprocesses in mesoporous silicas prepared by a supramolecular templating approach, J. Photochem. Photobiol., C, 3 (2002) 129–146.

[38] K. Hanna, I. Beurroies, R. Denoyel, D. Desplantier-Giscard, A. Galarneau, F. Di Renzo, Sorption of hydrophobic molecules by organic/inorganic mesostructures, J. Colloid Interface Sci., 252 (2002) 276–283.

[39] H. Zhao, K.L. Nagy, J.S. Waples, G.F. Vance, Surfactant-templated mesoporous silicate materials as sorbents for organic pollutants in water, Environ. Sci. Technol., 34 (2000) 4822–4827.

[40] M. Akyüz, D.J. Roberts, Determination of linear alkylbenzene sulphonates and their biodegradation intermediates by isocratic RP-HPLC, Turk. J. Chem., 26 (2002) 669–680.

[41] M. Zanjanchi, S. Asgari, Incorporation of aluminum into the framework of mesoporous MCM-41: the contribution of diffuse reflectance spectroscopy, Solid State Ionics, 171 (2004) 277–282.

[42] M. Koga, Y. Yamamichi, Y. Nomoto, M. Irie, T. Tanimura, T. Yoshinaga, Rapid determination of anionic surfactants by improved spectrophotometric method using methylene blue, Anal. Sci., 15 (1999) 563–568.

[43] L. Huang, Q. Huang, H. Xiao, M. Eić, Effect of cationic template on the adsorption of aromatic compounds in MCM-41, Microporous Mesoporous Mater., 98 (2007) 330–338.

[44] G. Vijayakumar, R. Tamilarasan, M. Dharmendirakumar, Adsorption, kinetic, equilibrium and thermodynamic studies on the removal of basic dye Rhodamine-B from aqueous solution by the use of natural adsorbent perlite, J. Mater. Environ. Sci., 3 (2012) 157–170.

[45] B. Nandi, A. Goswami, A. Das, B. Mondal, M. Purkait, Kinetic and equilibrium studies on the adsorption of crystal violet dye using kaolin as an adsorbent, Sep. Sci. Technol., 43 (2008) 1382–1403.

[46] A. Esposito, F. Pagnanelli, A. Lodi, C. Solisio, F. Veglio, Biosorption of heavy metals by *Sphaerotilus natans*: an equilibrium study at different pH and biomass concentrations, Hydrometallurgy, 60 (2001) 129–141.

[47] M.H. Dehghani, D. Sanaei, I. Ali, A. Bhatnagar, Removal of chromium(VI) from aqueous solution using treated waste newspaper as a low-cost adsorbent: kinetic modeling and isotherm studies, J. Mol. Liq., 215 (2016) 671–679.

[48] S. Nethaji, A. Sivasamy, A. Mandal, Adsorption isotherms, kinetics and mechanism for the adsorption of cationic and anionic dyes onto carbonaceous particles prepared from *Juglans regia* shell biomass, Int. J. Environ. Sci. Technol., 10 (2013) 231–242.

[49] W.B. Yang, A. Li, J. Fan, L. Yang, Q. Zhang, Adsorption of branched alkylbenzene sulfonate onto styrene and acrylic ester resins, Chemosphere, 64 (2006) 984–990.

[50] E. Fu, P. Somasundaran, C. Maltesh, Hydrocarbon and alcohol effects on sulfonate adsorption on alumina, Colloids Surf., A, 112 (1996) 55–62.